Science Advances
AAAS

advances.sciencemag.org/cgi/content/full/6/35/eaaz5752/DC1

Supplementary Materials for

SQR mediates therapeutic effects of H_2S by targeting mitochondrial electron transport to induce mitochondrial uncoupling

Jia Jia*, Zichuang Wang, Minjie Zhang, Caiyun Huang, Yanmei Song, Fuyou Xu, Jingyu Zhang, Jie Li, Meijun He, Yuyao Li, Guizhen Ao, Chengjiao Hong, Yongjun Cao, Y. Eugene Chin, Zi-chun Hua, Jian Cheng*

*Corresponding author. Email: jiajia@suda.edu.cn (J.J.); chengjian@suda.edu.cn (J.C.)

Published 26 August 2020, *Sci. Adv.* **6**, eaaz5752 (2020)
DOI: 10.1126/sciadv.aaz5752

This PDF file includes:

Supplementary Materials and Methods

Antibodies

The following antibodies were used: rabbit polyclonal anti-AMPKα (2532, dilution 1:1,000) and rabbit polyclonal anti-p-AMPKα (2535, dilution 1:1,000) antibodies from Cell Signaling Technology, rabbit polyclonal anti-SQR antibody (17256-1-AP, dilution 1:1,000) from Proteintech, rabbit polyclonal anti-CBS (sc-67154, dilution 1:1,000) and monoclonal anti-NDUFS3 (sc-374282, dilution 1:100) antibodies from Santa Cruz, monoclonal anti-β-actin antibody (ab008-100, dilution 1:1,000) from Multi Sciences, and monoclonal anti-GAPDH antibody (3781, dilution 1:5,000) from PROSCI.

Reagents

The following agents were purchased from Gibco: B27 supplement (17504-044), Neurobasal medium (21103049), DMEM (high glucose, C11995500BT), fetal bovine serum (FBS, 10099-141), glutamax (35050-061) and penicillin-streptomycin (15140122). DMEM/F12 (SH3002301) was purchased from Hyclone. The following agents were purchased from Sigma: dimethyl sulfoxide (DMSO, D4540), sodium hydrosulfide (NaHS, 161527), sodium pyruvate (S8636), poly-L-lysine solution (P4832), Coenzyme Q_{10} (C9538), Ampliflu^{TM} Red (90101), diethyl succinate (112402), peroxidase from horseradish (P8375), FCCP (C2920), rotenone (R8875), zinc chloride ($ZnCl_2$, 31650), ADP/ATP Ratio Assay Kit (MAK135), Lactate Assay Kit (MAK064), tetramethylrhodamine methyl ester perchlorate (TMRM, T5428), MitoTEMPO (SML0737), Coenzyme Q_4 (C2470) and Hoechst 33342 (B2261). Methanol (A452-4), ammonium formate (A115-50) and hexanes (H303-4) were

purchased from Fisher Chemical. Coenzyme Q_9 (158165) was purchased from J&K Scientific. The following agents were purchased from Thermo Fisher Scientific: MitoSOX Red (M36008), Mitotracker Green (M7514), protein ladder (26616), Pierce™ BCA Protein Assay Kit (23227), enhanced chemiluminescent (ECL) western blotting reagents (SuperSignal West Pico, Pierce, 34077), mouse IL-1β uncoated ELISA Kit (88-7013-88), mouse TNF-α uncoated ELISA Kit (88-7324-88) and High Capacity cDNA Reverse Transcription Kit (4368813). Sodium chloride (A610476-0001) and non-fat powdered milk (A600669-0250) were purchased from BBI Life Sciences. Sodium dihydrogen phosphate dihydrate (20040718), disodium hydrogen phosphate (10020318), hydrochloric acid (10011018) and ethylenediamine tetraacetic acid (10009617) were purchased from Sinopharm Chemical Reagent Co., Ltd. Ammonium persulfate (A600072), glycine (A502065-0500), SDS (A500228-0250) and Tris (A501492) were purchased from Sangon Biotech. Propanol (P110345) and genipin (G101204) were purchased from Aladdin. Superoxide dismutase (S0086), RIPA lysis buffer (P0013B) and mitochondrial membrane potential assay kit with JC-1 (C2006-1) were purchased from Beyotime. RNAprep Pure Micro Kit (DP420) and RNAprep Pure Tissue Kit (DP431) were purchased from TIANGEN Biotech. Puromycin (REVG1001) was purchased from GeneChem. SYBR qPCR Master Mix (Q331-02) was purchased from Vazyme. NAD/NADH-Glo™ Assay (G9071) was purchased from Promega. Complex IV activity assay kit (K287-100) was purchased from Biovision. Seahorse XFe24 FluxPaks (102342-100), Seahorse XF Cell Mito Stress Test Kit (containing oligomycin and antimycin A, 103015-100), XF Calibrant Solution (100840-000) and XF Base Medium (102353-100) were purchased from Agilent Technologies.

Synthesis of ADT-OH and treatment with H_2S donors

The slow-releasing organic H_2S donor ADT-OH [5-(4-hydroxyphenyl)-3H-1,2-dithiole-3-thione] was prepared from ADT [5-(4-methoxyphenyl)-3H-1,2-dithiole-3-thione]. ADT, also known as anethol trithione, is a clinical drug and was purchased from Huanggang Saikang Pharmaceutical Co., Ltd. (Hubei province, China). The molecular structure of ADT-OH was determined using ^{1}H NMR spectra with a Varian Unity Inova 400/600 MHz NMR Spectrometer and referenced to TMS. δ (ppm, DMSO - d_6): 10.46 (s, 1H, OH), 7.77 (d, 2H, *J* = 8.7 Hz, ArH), 7.68 (s, =CH), 6.89 (d, 2H, *J* = 8.7 Hz, ArH). The purity of ADT-OH was determined with analytical HPLC (SHIMADZU LC-20AD). The slow releasing organic H_2S donor 5a [N-(Benzoylthio) benzamide] (*21*) was purchased from Dojindo Laboratories (Mashikimachi, kamimashiki gun Kumamoto, Japan). For *in vitro* studies, the organic H_2S donors were dissolved in DMSO and NaHS in water, and then were added to medium to desired concentrations. For *in vivo* administration, ADT-OH was dissolved in DMSO, followed by dilution with corn oil (10% DMSO in corn oil). ADT-OH were administered via the intraperitoneal route at the dose of 50 mg/kg/day.

Primary and cell line cultures

Primary microglia were prepared from 1-day-old newborn mice, and primary cortical neurons were prepared from 16-day mouse embryos. We also used murine BV2 microglia. BV2 cell line was generated by infecting primary mouse microglia with retrovirus (J2) carrying a v-raf/v-myc oncogene, and has been characterized to be a suitable alternative model for primary microglia. Primary microglia and murine BV2 microglia were cultured in

DMEM supplemented with 10% (v/v) FBS at 37 °C and 5% CO_2. Primary neurons were cultured in neurobasal medium supplemented with 2% B27 and 1% glutamax. The purity of primary cell cultures was assessed by qPCR measurement of mRNA levels of the microglial marker (CD11b), astrocytic marker (GFAP) and neuronal marker (NeuN).

RNA interference in the BV2 microglia

The small interference RNA (siRNAs, 0.5 μg/mL) targeting murine SQR, AMPKα1/α2, or UCP2 was transfected into BV2 microglia using Entranster^{TM}-R per the manufacturer's instructions (Engreen, Beijing, China). At 48 h after transfection, cells were used for examination of the knockdown efficiencies or for further experiments. A nonsense siRNA (Ctrl-siRNA) that did not target any mammalian DNA sequence served as the negative control. siRNAs were synthesized by Genepharma (Shanghai, China). Murine SQR siRNA (5'-*GACGAGAACUGUAUCCGCA*tt-3') has been validated in a previous study (*39*). The siRNA targeting murine AMPKα1/α2 (5'-*GAGAAGCAGAAGCACGACG*tt-3') has been successfully used by our group to knock down AMPK in BV2 microglia (*19*). The siRNA against murine UCP2 (5'-CGUAGUGAUGUUUGUCACCtt-3') was used in the study.

Lentiviral infection of primary microglia, primary neurons and HEK293 cells

Primary neurons and microglia were infected with lentivirus for 4 days in culture prior to further experiments. Specifically, mouse primary cortical neurons at 6 days after culture *in vitro* were infected with the lentivirus co-expressing murine SQR cDNA (NM_001162503) and enhanced green fluorescent protein (eGFP). The lentiviral vector expressing eGFP only

was used as the control. Murine SQR cDNA was synthesized, and lentivirus expressing SQR cDNA was constructed by Genechem (Shanghai, China). For knockdown of SQR in mouse primary microglia, SQR specific shRNA (5'- *TGGACTATGAGAAGATTAA* TTCAAGAGA *TTAATCTTCTCATAGTCCA* TTTTT -3') was packaged into lentivirus by Genechem (Shanghai, China). Primary microglia were seeded on 24-well plates at the density of 10^5 cells/well and infected with lentivirus expressing SQR shRNA. Lentivirus expressing a non-sense shRNA (Ctrl shRNA) that did not target any mammalian DNA sequence served as the negative control (From Genechem Inc., Shanghai, China). At 4 days after infection, neurons or microglia were used for further experiments. The siRNA sequence against NDUFS3 [NADH dehydrogenase (ubiquinone) Fe-S protein 3], a subunit of complex I, has been validated (*40*). For knockdown of NDUFS3 in HEK293 cells, NDUFS3 shRNA (5'- *TCCATCACCATCTTCCAG* TTCAAGAGA *ATGAGTCCTTCCACGATACC* -3') was designed based on the reported siRNA sequence and packaged into lentivirus by Genechem (Shanghai, China). HEK293 cells were seeded onto 24-well plates at the density of 10^5 cells/well and infected with lentivirus expressing NDUFS3 shRNA or Ctrl shRNA. At 2 days after infection, HEK293 cells were used for further experiments, including western blot analysis of knockdown efficiency and assessment of $\Delta\Psi_m$, ADP/ATP ratios and OCR.

Assessment of the mitochondrial membrane potential ($\Delta\Psi_m$)

The fluorescent probes JC-1 and TMRM were used to stain cultured cells to indicate $\Delta\Psi_m$ as reported (*17*). JC-1 diffuses from the mitochondria into the plasma when the mitochondrial membrane potential decreases, as indicated by the shift in fluorescence

emission from red (Excitation at 579 nm/Emission at 599 nm) to green (Excitation at 485 nm/Emission at 516 nm). For JC-1 staining, cells were seeded on 24-well plates at the density of 10^5 cells/well. Before the assay, cells were treated with different chemicals for the indicated periods of time as indicated. Then, JC-1 was added at a final concentration of 100 nM to stain cells for 10 min. After cells were washed twice with PBS, fluorescence was visualized using confocal microscopy (Zeiss LSM700, Germany) with constant parameters to acquire all images. The ratio of the red/green mean fluorescence intensity was assessed semi-quantitatively using ImageJ software (http://rsbweb.nih.gov/ij/). To analyze the mitochondrial membrane potential with TMRM, cells were seeded on 24-well plates. Cells were treated with H_2S donors and/or rotenone (10 nM), $ZnCl_2$ (800 μM), the mitochondria-targeted ROS scavenger MitoTEMPO (1.5 mM) or UCP2 inhibitor genipin (20 nM) for the indicated periods of time. After washing with PBS, cells were stained with TMRM for 10 min at a final concentration of 100 nM. Fluorescence was visualized under confocal microscopy (Zeiss LSM700, Germany) by excitation at 560 nm and emission above 575 nm with the constant parameters to acquire all images. For some experiments, TMRM fluorescence was also quantitatively assayed with a microplate reader. Briefly, BV2 microglia or HEK293 cells were seeded on 96-well plates at the density of 10^4 cells/well. After cells were treated as indicated, TMRM (100 nM) was added to stain cells for 10 min. After washing with PBS, TMRM fluorescence was determined by excitation at the 560 nm and emission at 575 nm with Infinite M1000 Pro Reader (TECAN, Ma¨nnedorf, Switzerland).

Measurement of relative sulfide levels in culture medium of HEK293 cells

To investigate whether CBS overexpression enhanced endogenous production of H_2S, we measured relative sulfide levels in culture medium collected from HEK293 cells, as reported previously (*19*). Briefly, wild-type HEK293 cells (WT HEK), control HEK293 cells stably infected with control lentivirus expressing eGFP (Ctrl HEK), and HEK293 cells stably infected with lentivirus expressing CBS and eGFP (CBS HEK) were cultured in phenol red-free medium overnight. Then, the medium was collected for assessment of sulfide levels. HEK293 cells were also harvested for measurement of cellular protein concentrations with a BCA protein assay kit. The collected medium (500 μL) was mixed with zinc acetate (1% w/v, 250 μL). Then, 133 μL of N, *N*-dimethyl-p-phenylenediamine sulfate (20 μM) in 7.2 mol/L HCl and $FeCL_3$ (30 μM; 133 μL) in 1.2 mol/L HCL were added to the mixture, followed by addition of 10% trichloroacetic acid (250 μL) to precipitate proteins. After centrifugation at 24,000 g for 5 min at 4°C, supernatants were collected and the absorbance was measured at 670 nm with infinite 2000 PRO (TECAN, Ma¨nnedorf, Switzerland). The sulfide level for each sample was calculated against a calibration curve generated with NaHS standard. Final sulfide levels were normalized to the cellular protein concentrations and expressed as the percentage of sulfide levels in the medium collected from wild-type HEK293 cells (% WT HEK).

Determination of ATP levels and ADP/ATP ratios

To indicate mitochondrial uncoupling in cultured cells, cellular ATP and ADP were assessed at 30 min after the treatment with uncouplers unless otherwise noted. The ADP/ATP

ratio assay kit was used to measure cellular ATP and ADP. Cells were seeded on a 96-well microplate (10^4 cells/well). Cells were treated with the H_2S donors or classic uncouplers at the indicated concentrations with/without rotenone (10 nM) or $ZnCl_2$ (800 μM). Control cells were treated with vehicle. The assay of ATP and ADP was performed per the manufacturer's manual. Luminescence was measured with an Infinite M1000 Pro Reader (TECAN, Ma¨nnedorf, Switzerland). ADP/ATP ratios were calculated according to the manual. The final results of ATP levels were expressed as the percentages of the ATP levels of the control cells treated with vehicle. For recombinant HEK293 cells, results were presented as the percentages of ATP levels of wild-type HEK293 cells.

Western blotting

Cells or tissues were homogenized in RIPA lysis buffer supplemented with mini-complete protease inhibitor cocktail and phosphatase inhibitor cocktail for 30 min on ice. After centrifugation at 13,200 rpm for 25 min, supernatants were collected and stored at −20 °C. Protein concentrations were assessed with a BCA kit. For each sample, 30 μg proteins were subjected to SDS-PAGE gels. Briefly, cell extracts were mixed with 5× Laemmli loading buffer and then heated for 5 min at 100 °C. After electrophoresis on 12% SDS-PAGE gels, proteins were transferred to polyvinylidene difluoride (PVDF) membranes. PVDF membranes were blocked in PBS supplemented with 5% non-fat milk and 0.1% Tween-20 for 1 h at room temperature. Membranes were then incubated with the following primary antibodies followed by appropriate secondary antibodies: rabbit polyclonal anti-AMPKα, rabbit polyclonal anti-p-AMPKα, rabbit polyclonal anti-SQR, rabbit polyclonal anti-CBS, mouse monoclonal

anti-NDUFS3, and anti-UCP2 antibodies. To visualize protein bands, chemiluminescent detection was performed using enhanced chemiluminescent (ECL) western blotting reagents. For semi-quantification, protein band intensities were assayed using ImageJ software. The final results were expressed as the ratios of the protein of interest to an internal loading control or total protein.

Isolation of functional mitochondria from cultured cells

Functional mitochondria were isolated from BV2 microglia or primary neurons, and used for determination of H_2O_2 generation and NAD^+/NADH ratios. Briefly, cells were cultured on 10-cm dishes to reach 80% confluence. Medium was removed and cells were washed once with PBS. Then, cells were detached and transferred to a tube. Cell suspension was centrifuged at 600 g for 10 min at 4 °C. Cell pellets were re-suspended in 3 mL of ice-cold isolation buffer that contained 0.01 M Tris–MOPS, 1 mM EGTA/Tris and 0.2 M sucrose. Then, cells were homogenized, and homogenates were centrifuged at 600g for 10 min at 4 °C to remove cellular debris. Supernatants were collected and centrifuged at 7,000g for 10 min at 4 °C. Pellets were collected and re-suspended in 200 μL ice-cold isolation buffer. Finally, pellets containing functional mitochondria were obtained by centrifugation at 7,000g for 10 min at 4 °C.

Measurement of NAD^+/NADH ratios in isolated mitochondria

Functional mitochondria were isolated from BV2 microglia. Mitochondria were resuspended in 50 μL buffer containing 0.01 M Tris–MOPS, 1 mM EGTA/Tris and 0.2 M

sucrose, and treated with ADT-OH and/or rotenone for 10 min. Then, a base buffer (0.2 M sodium hydroxide supplemented with 1% dodecyltrimethylammonium bromide) was added to lyse mitochondria. The ratio of NAD^+/NADH was assayed per the manufacturer's instructions (Promega).

Determination of the H_2S-releasing kinetics of H_2S donors

BV2 microglia were seeded on 10-cm dishes and cultured overnight. Then, culture medium was replaced with fresh medium, followed by addition of ADT-OH, 5a or NaHS. Medium (500 μL) was collected at the indicated timepoints following addition of the H_2S donors. Intact medium served as the blank control. Medium was mixed with zinc acetate (1% w/v, 250 μL) immediately. Then, 133 μL of N, *N*-dimethyl-p-phenylenediamine sulfate (20 μM) in 7.2 mol/L HCl and 133 μL of $FeCL_3$ (30 μM) in 1.2 mol/L HCl were added to the mixture, followed by addition of 10% trichloroacetic acid (250 μL) for protein precipitation. After centrifugation at 24,000 g for 5 min at 4°C, supernatants were collected and the absorbance was measured at 670 nm with infinite 2000 PRO (TECAN, Ma¨nnedorf, Switzerland). After subtracting the absorbance of the blank control from the absorbance of each sample, the sulfide concentration for each sample was calculated from a calibration curve generated with NaHS standard. Results were expressed in μM.

Mitochondrial swelling assay

Mitochondria were isolated from the livers of global SQR knockout mice ($Sqr^{-/-}$) before 2-month-old. Livers were homogenized with a Downs homogenizer on ice, and resuspended

with ice-cold isolation buffer containing 225 mM mannitol, 75mM sucrose and 10mM Tris-HCl (pH 7.4). Homogenates were centrifuged at 600 g for 10 min to remove tissue debris. Supernatants were collected and centrifuged at 7,000 g for 10 min. Pellets containing mitochondria were collected and resuspended in isolation buffer. The procedure was repeated once. Mitochondrial swelling assay was carried out by adding mitochondria to the isotonic buffer containing 5 mM Tris-HCl (pH 7.4), 145 mM potassium acetate, 0.5 mM EDTA, 3 μM valinomycin and 1 μM rotenone, followed by addition of ADT-OH (50 μM), FCCP (1 μM) or vehicle at the indicated timepoint. The absorbance of the mitochondrial suspension at 600 nm was continually monitored following addition of mitochondria using a microplate reader (TECAN, Ma¨nnedorf, Switzerland). The decrease in the absorbance indicated swelling of mitochondria.

Lactate assay

Lactate accumulation was assessed in BV2 microglia treated with ADT-OH and/or rotenone for 2 h by measuring lactate levels in culture medium, as reported previously (*27*). The assay was performed using a colorimetric kit according to the manufacturer's instructions.

Neuronal viability assay

Neuronal viability was assessd with a WST-8-based kit (C0037, Biyuntia, China). WST8, a tetrazolium salt, is bio-reduced by cellular dehydrogenases to an orange formazan product that is soluble in culture medium. The amount of formazan produced is directly proportional to the number of living cells. Mouse primary neurons seeded on 96-well plates were cultured

in vitro for 10 days and then incubated with ADT-OH, 5a or vehicle for 2 h. After assay solution (10 μl) was added to each well, plates were incubated at 37ºC for additional 0.5 h. Optical absorbance at 450 nm, which was directly proportional to the number of living neurons, was determined for each well and expressed as a percentage of control neurons treated with vehicle.

Intrastriatal microinjection of lentivirus

All animal procedures were approved by the Committee on Use and Care of Animals, Soochow University. Two-month-old male ICR mice were purchased from Shanghai SLAC Laboratory Animal Co., Ltd. (Shanghai, China). Lentivirus was injected into the left striatum under anesthesia. Briefly, mice were placed onto a stereotaxic apparatus (Model 500, Kopf Instruments, Tujunga, CA, USA). A small hole was drilled through the skull. Concentrated lentivirus expressing SQR shRNA or nonsense shRNA (Genechem Inc., Shanghai, China) were injected into the two positions in the left striatum at a rate of 0.5 μL/min with a 30-gauge needle on a 2-μL Hamilton syringe (1 μL per site). The coordinates of the injection sites were: 0.5 mm anterior to the bregma, 2.0 mm lateral to the midline and 3.5 mm below the skull; and 1 mm anterior to the bregma, 1.5 mm lateral to the midline and 3.2 mm below the skull. At 14 days after injection, the in vivo knockdown efficiency was assessed by western blot analysis of brain tissue extracted from the striatum. The mice were subjected to intracerebral hemorrhage (ICH) as described below at 14 days after lentiviral injection.

Enzyme-linked immunosorbent assay (ELISA)

Commercial ELISA kits (Thermo Fisher Scientific) were used to measure concentrations of IL-1β, Il-6 and TNF-α in culture medium or striatal tissue extracted from mice at 3 days following ICH. Briefly, primary microglia or BV2 microglia were seeded on 24-well plates at the density of 10^5 cells/well. Before the assay, microglia were treated with lysate of red blood cells and/or ADT-OH for 24 h. Then, medium was harvested for ELISA measurement. For tissue samples, brain tissue was harvested from the ipsilateral (hemorrhagic) striatum as well as the contralateral striatum at 3 days following ICH, and used for ELISA measurement of IL-1β, Il-6 and TNF-α protein levels. Protein concentrations of tissue samples were also determined with a commercial BCA kit. The levels of IL-1β, TNF-α, and IL-6 were assessed per the manufacturer's instructions. Optical absorbance was measured at 450 nm using Infinite M1000 Pro Reader (TECAN, Ma¨nnedorf, Switzerland). The concentrations of IL-1β, Il-6 and TNF-α were calculated from a calibration curve made with IL-1β, Il-6 or TNF-α standard samples. Results were normalized to protein concentrations, or expressed in pg/ml supernatant for cultured microglia.

Real-time quantitative RT-PCR (qPCR)

For qPCR assay of mRNA levels of pro-inflammatory markers, microglia were collected at 6 h after treatment with lysate of red blood cells. Mouse primary microglia, astrocytes and neurons were cultured as described above and collected for determination of SQR mRNA expression. Total RNA was extracted from cells using the RNAprep pure Micro Kit (TIANGEN Biotech, Beijing, China). The concentrations of total RNA were quantified using

Nanodrop 2000. cDNA was synthesized from 20 ng total RNA using a High-Capacity cDNA Reverse Transcription Kit. Real-time qPCR was performed with cDNA using a SYBR green technique on the 7500 Sequence Detection System. qPCR primers were synthesized by Sangon Biotech. Sequences of primers are as follows: mouse *18s* (forward: 5´-TCAACACGGGAAACCTCAC-3´; reverse: 5´-CGCTCCACCAACTAAGAAC-3´); mouse *IL-6* (forward: 5´-GAGGATACCACTCCCAACAGACC-3´; reverse: 5´-AAGTGCATCATCGTTGTTCATACA-3´); and mouse *Sqr* (forward: 5´-GGATTCAAGATAGAGTGGCGG-3´; reverse: 5´-AGCAAAGCCTTCAGGTAGTC-3´). Results were normalized to *18s* RNA levels and expressed as the ratios to control cells.

Assessment of brain edema in mice following ICH.

Brains were harvested at 3 days after ICH, and the left and right striatum were dissected and harvested. Wet weight of the harvested striatal tissue was determined. Then, the dry weight of the tissue was weighed after tissue samples were kept in an oven at 80°C for 48 h. Edema was assessed according to the following formula: (wet weight – dry weight)/ wet weight. The results were expressed as the percentages of wet weight.

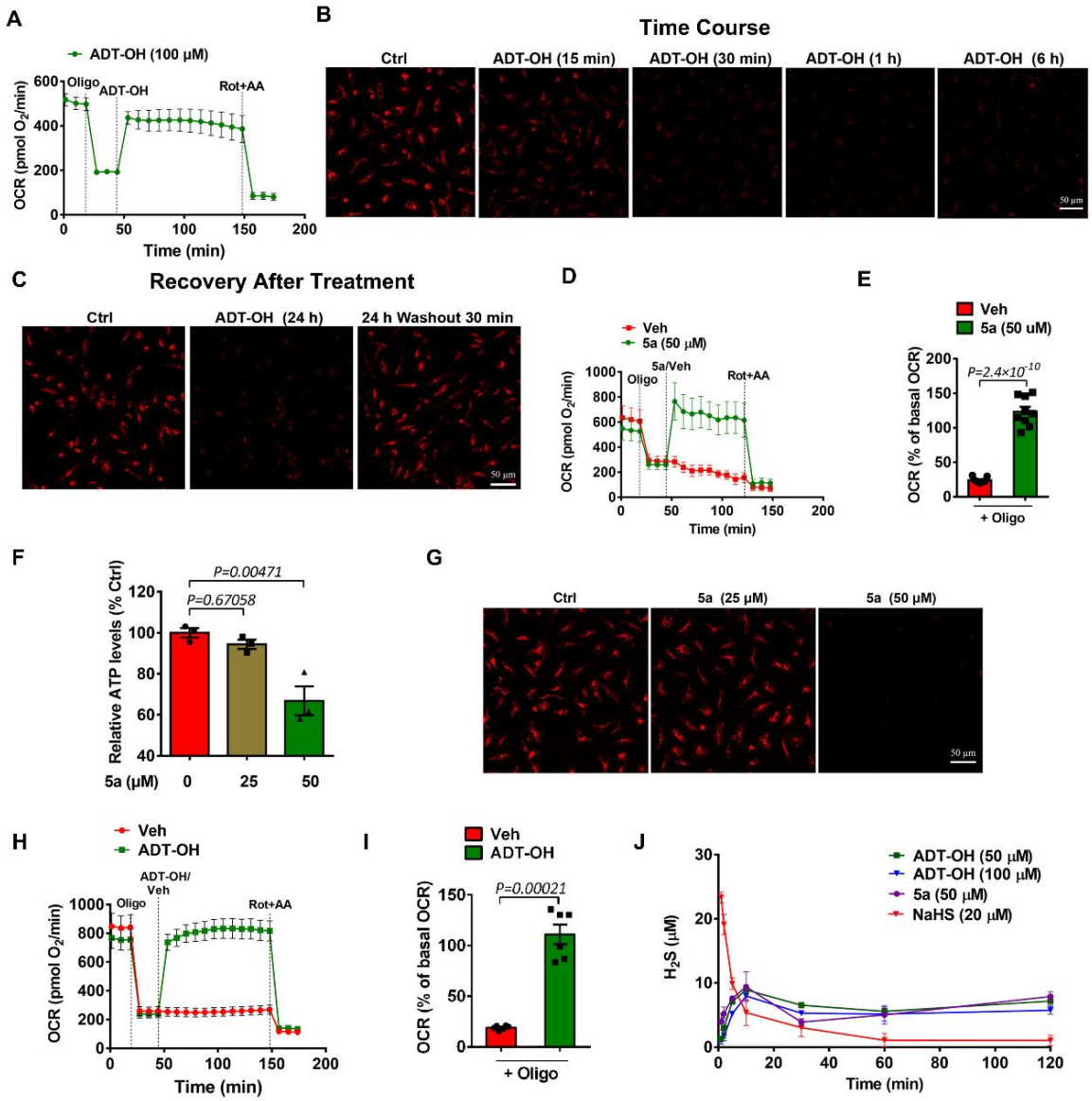
A
ADT-OH (100 μM)
Oligo
ADT-OH
Rot+AA
OCR (pmol O2/min)
Time (min)
B
Time Course
Ctrl
ADT-OH (15 min)
ADT-OH (30 min)
ADT-OH (1 h)
ADT-OH (6 h)
50 μm
C
Recovery After Treatment
Ctrl
ADT-OH (24 h)
24 h Washout 30 min
50 μm
D
Veh
5a (50 μM)
5a/Veh
Oligo
Rot+AA
OCR (pmol O2/min)
Time (min)
E
Veh
5a (50 uM)
P=2.4×10-10
OCR (% of basal OCR)
+ Oligo
F
P=0.00471
P=0.67058
Relative ATP levels (% Ctrl)
5a (μM) 0 25 50
G
Ctrl
5a (25 μM)
5a (50 μM)
50 μm
H
Veh
ADT-OH
ADT-OH/ Veh
Oligo
Rot+AA
OCR (pmol O2/min)
Time (min)
I
Veh
ADT-OH
P=0.00021
OCR (% of basal OCR)
+ Oligo
J
ADT-OH (50 μM)
ADT-OH (100 μM)
5a (50 μM)
NaHS (20 μM)
H2S (μM)
Time (min)

Fig. S1. H_2S donors induce mitochondrial uncoupling. (**A**) Real-time change of OCR (n = 6) in primary microglia treated with the H_2S donor ADT-OH (100 μM). Oligomycin (Oligo), rotenone (Rot) and antimycin A (AA) were added at the indicated timepoints. (**B-C)** Time course of mitochondrial uncoupling induced by ADT-OH in primary microglia, as indicated by TMRM staining of primary microglia treated with 50 μM ADT-OH for the indicated periods of time (B) or treated with 50 μM ADT-OH for 24 h followed by incubation in ADT-OH-free medium for 30 min (C), 3 independent replicates. (**D-G**) Induction of mitochondrial uncoupling by the H_2S donor 5a at 50 μM in primary microglia, as indicated by enhanced OCR in the presence of oligomycin (D, real-time change; E, statistical analysis; n = 9), reduced intracellular ATP levels (F, n = 3), and reduced $\Delta\Psi_m$ (G, TMRM staining, 3 independent replicates). Ctrl: cells treated with vehicle. ATP/ADP and $\Delta\Psi_m$ were assessed at 30 min after 5a treatment. (**H-I**) Induction of mitochondrial uncoupling by ADT-OH (50 μM) in BV2 microglia, as indicated by enhanced OCR in the presence of oligomycin (I: real-time change; J: statistical results; n = 6). (**J**) The H_2S-releasing kinetics of the organic donors (ADT-OH and 5a) and the inorganic donor (NaHS).

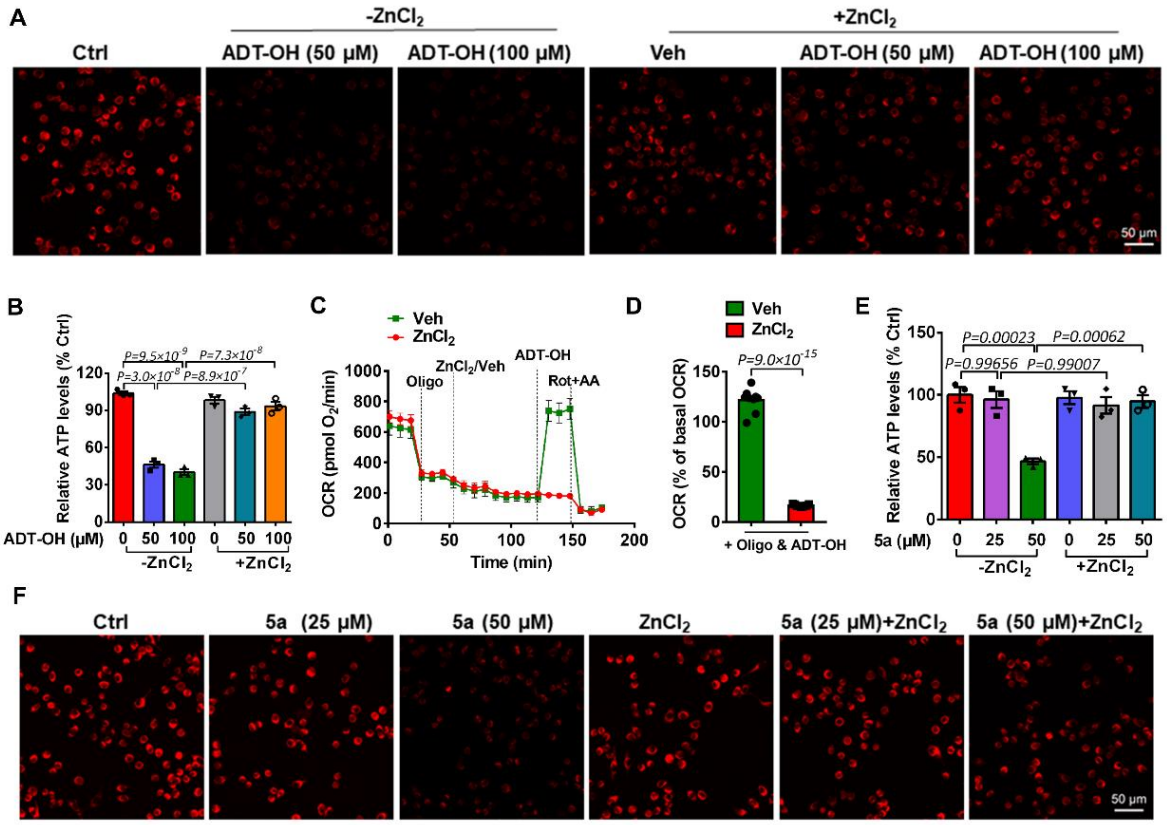

Fig. S2. H_2S donors induce mitochondrial uncoupling via H_2S. (**A**) $\Delta\Psi_m$ in BV2 microglia, as assessed by TMRM staining of cells at 30 min of treatment with ADT-OH in the presence or absence of $ZnCl_2$ (3 independent replicates). Ctrl: cells treated with vehicle. $ZnCl_2$ (800 μM) was added to block the effects of free H_2S. (**B**) Intracellular ATP levels in BV2 microglia at 30 min after treatment with ADT-OH in the presence or absence of $ZnCl_2$ (n = 3). (**C-D**) $ZnCl_2$ blocked ADT-OH-induced increase in OCR in the presence of oligomycin (C: real-time changes of OCR; D: statistical analysis, n = 9). (**E**) Intracellular ATP levels in BV2 microglia treated with 5a and/or $ZnCl_2$ for 30 min (n = 3). (**F**) $\Delta\Psi_m$ in BV2 microglia treated with 5a and/or $ZnCl_2$ for 30 min (TMRM staining, 3 independent experiments).

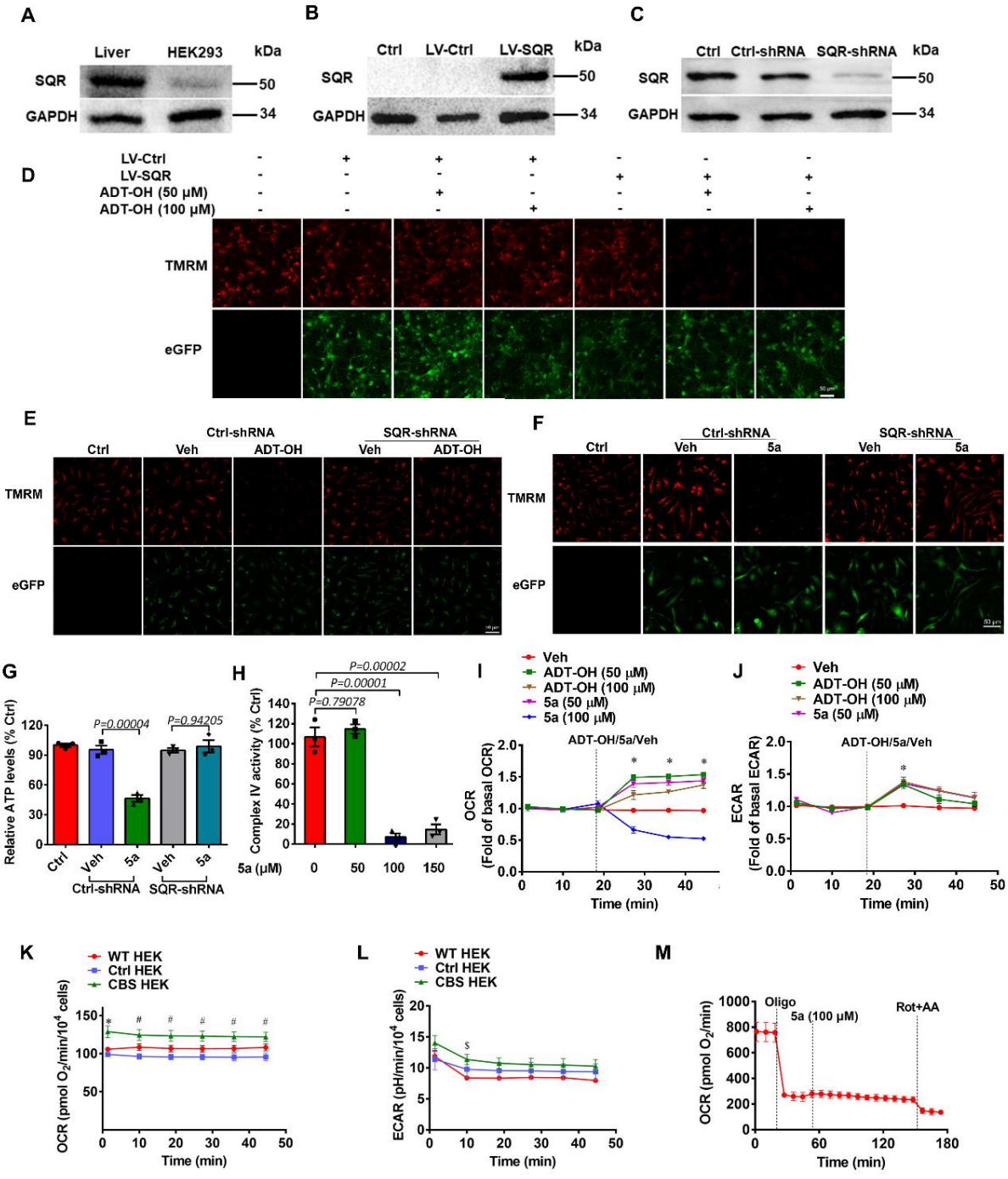
A
Liver
HEK293
kDa
SQR
GAPDH
50
34
B
Ctrl
LV-Ctrl
LV-SQR
kDa
SQR
GAPDH
50
34
C
Ctrl
Ctrl-shRNA
SQR-shRNA
kDa
SQR
GAPDH
50
34
D
LV-Ctrl
LV-SQR
ADT-OH (50 μM)
ADT-OH (100 μM)
TMRM
eGFP
E
Ctrl-shRNA
SQR-shRNA
Ctrl
Veh
ADT-OH
Veh
ADT-OH
TMRM
eGFP
F
Ctrl
Ctrl-shRNA
Veh
5a
SQR-shRNA
Veh
5a
TMRM
eGFP
G
Relative ATP levels (% Ctrl)
P=0.00004
P=0.94205
Ctrl
Veh
5a
Veh
5a
Ctrl-shRNA
SQR-shRNA
H
Complex IV activity (% Ctrl)
P=0.00002
P=0.00001
P=0.79078
5a (μM)
0
50
100
150
I
Veh
ADT-OH (50 μM)
ADT-OH (100 μM)
5a (50 μM)
5a (100 μM)
ADT-OH/5a/Veh
OCR (Fold of basal OCR)
Time (min)
J
Veh
ADT-OH (50 μM)
ADT-OH (100 μM)
5a (50 μM)
ADT-OH/5a/Veh
ECAR (Fold of basal ECAR)
Time (min)
K
WT HEK
Ctrl HEK
CBS HEK
OCR (pmol O2/min/10^4 cells)
Time (min)
L
WT HEK
Ctrl HEK
CBS HEK
ECAR (pH/min/10^4 cells)
Time (min)
M
Oligo
5a (100 μM)
Rot+AA
OCR (pmol O2/min)
Time (min)

Fig. S3. H_2S-induced mitochondrial uncoupling requires SQR and is separable from the inhibition of complex IV by H_2S. (**A**) Expression of SQR protein in HEK293 cells. Liver: positive control. (**B**) SQR expression in primary neurons infected with lentivirus expressing SQR and eGFP (LV-SQR) for 4 days. Ctrl: non-infected cells; LV-Ctrl: lentivirus expressing eGFP. (**C**) Knockdown efficiency of SQR in primary microglia infected with lentivirus co-expressing SQR-shRNA and eGFP (SQR-shRNA) for 4 days. Ctrl-shRNA: control lentivirus co-expressing nonsense shRNA and eGFP. (**D**) TMRM staining of primary neurons infected with LV-SQR or LV-Ctrl for 4 days and then treated with ADT-OH for 30 min (3 independent experiments). (**E-F)** TMRM staining of primary microglia infected with SQR-shRNA or ctrl-shRNA for 4 days and then treated with 50 μM ADT-OH or 50 μM 5a for 30 min (3 independent experiments). Veh: vehicle. (**G**) Intracellular ATP levels (n = 3) in primary microglia infected with SQR-shRNA or ctrl-shRNA for 4 days and then treated with 5a (50 μM) or Veh for 30 min. (**H**) Complex IV activity in BV2 microglia treated with 5a for 30 min (n = 4). (**I-J**) The effects of ADT-OH and 5a on basal OCR and ECAR of BV2 microglia. ADT-OH, 5a or vehicle were added at the indicated timepoint. *: $p < 0.05$, H_2S donors vs. Veh. (K-L) Basal OCR and ECAR of wild-type HEK293 cells (WT HEK), control HEK293 cells (Ctrl HEK) and HEK293 cells overexpressing CBS (CBS HEK). *: $p < 0.05$ CBS HEK vs. WT HEK or Ctrl HEK. #: $p < 0.05$, CBS HEK vs. Ctrl HEK. $: $p < 0.05$, CBS HEK vs. WT HEK. (**M**) OCR in BV2 microglia treated with 100 μM 5a (I, n = 3). Oligomycin (Olig), rotenone (Rot) and antimycin (AA) were added at the indicated timepoints.

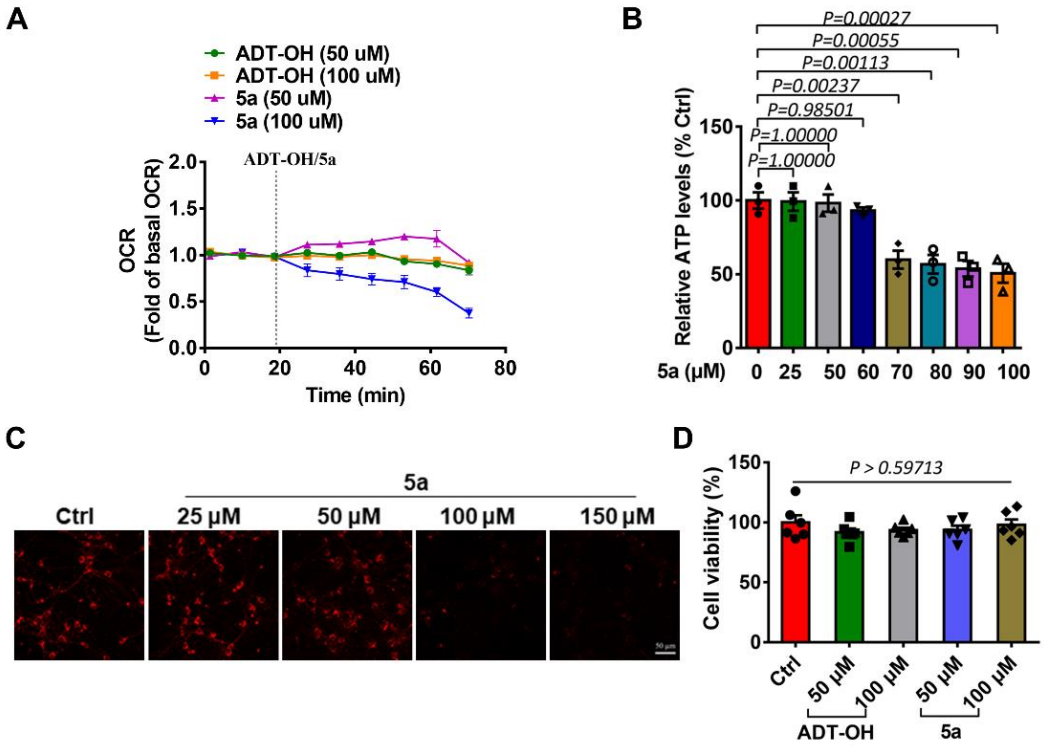

Fig. S4. The H_2S donor 5a reduces basal OCR and ATP levels in neurons at high concentrations. (**A**) The effects of 5a and ADT-OH on basal OCR of primary neurons. ADT-OH and 5a were added at the indicated timepoint (n = 9). (**B**) Intracellular ATP levels in primary neurons at 30 min after treatment with 5a (n = 3). **(C)** TMRM staining of primary neurons at 30 min of treatment with 5a, 3 independent replicates. (**D**) The viability of primary neurons incubated with 5a or ADT-OH for 2 h.

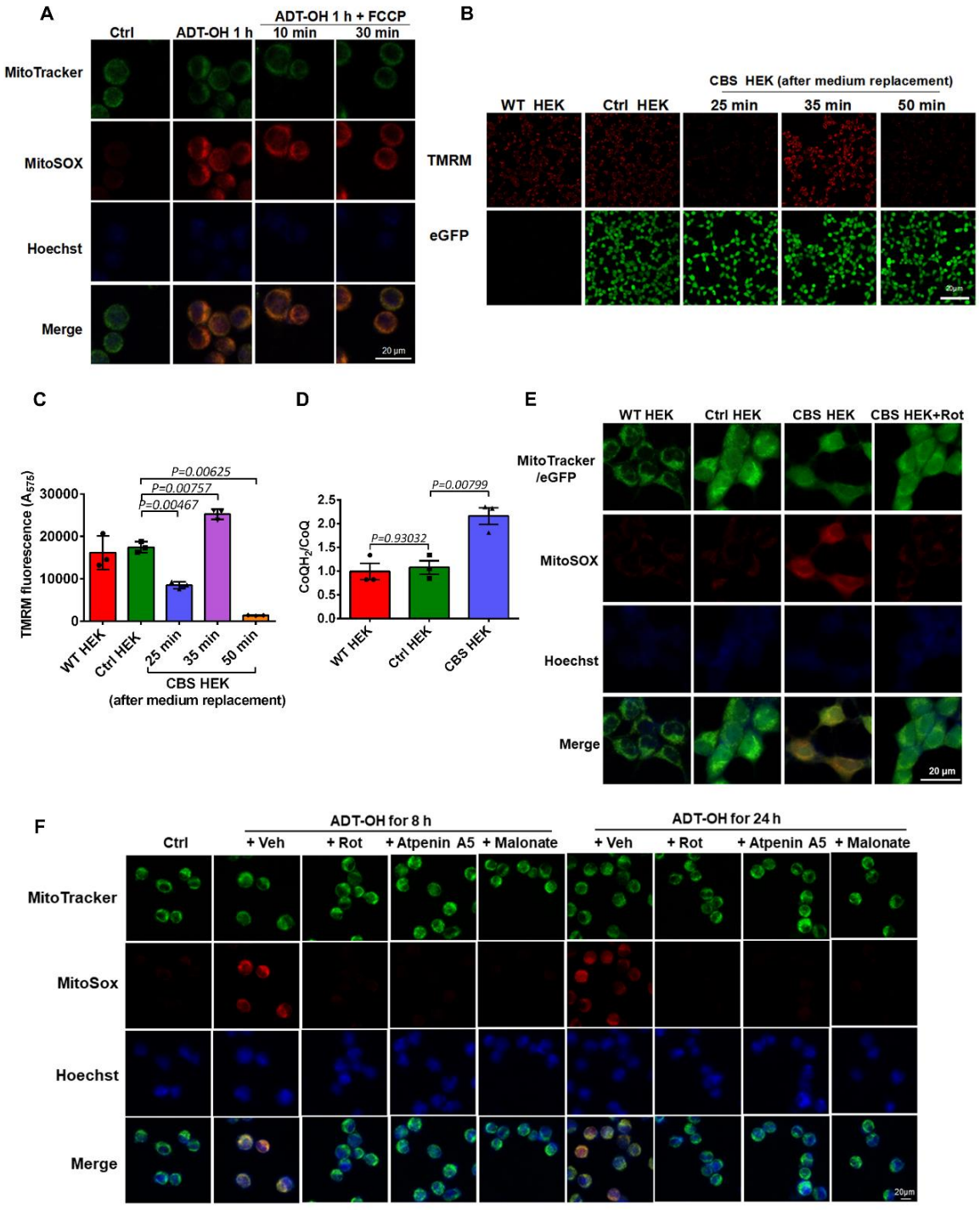
A
Ctrl
ADT-OH 1 h
ADT-OH 1 h + FCCP
10 min
30 min
MitoTracker
MitoSOX
Hoechst
Merge
20 μm
B
CBS HEK (after medium replacement)
WT HEK
Ctrl HEK
25 min
35 min
50 min
TMRM
eGFP
20μm
C
TMRM fluorescence (A575)
P=0.00625
P=0.00757
P=0.00467
30000
20000
10000
0
WT HEK
Ctrl HEK
25 min
35 min
50 min
CBS HEK
(after medium replacement)
D
CoQH2/CoQ
P=0.00799
P=0.93032
2.5
2.0
1.5
1.0
0.5
0.0
WT HEK
Ctrl HEK
CBS HEK
E
WT HEK
Ctrl HEK
CBS HEK
CBS HEK+Rot
MitoTracker /eGFP
MitoSOX
Hoechst
Merge
20 μm
F
ADT-OH for 8 h
ADT-OH for 24 h
Ctrl
+ Veh
+ Rot
+ Atpenin A5
+ Malonate
+ Veh
+ Rot
+ Atpenin A5
+ Malonate
MitoTracker
MitoSox
Hoechst
Merge
20μm

Fig. S5. H_2S drives complex I RET. (**A**) Mitochondrial ROS levels in BV2 microglia treated with ADT-OH (50 μM) for 1 h and then treated with FCCP (20 nM) for the indicated periods of time (MitoSOX staining from 3 independent replicates). (**B-C**) Time course of the change in $\Delta\Psi_m$ of overnight cultured CBS HEK (HEK293 cells overexpressing CBS and eGFP) after replacement of overnight culture medium with fresh medium (B, representative images of TMRM staining; C, quantification with a microplate reader, n = 3). Ctrl HEK: control HEK293 cells expressing eGFP. (**D**) $CoQH_2$/CoQ ratios in WT HEK, Ctrl HEK and CBS HEK (n = 3). (**E**) Mitochondrial ROS levels in WT HEK, Ctrl HEK and CBS HEK cells with/without Rot (3 independent replicates). Green: MitoTracker Green fluorescence for WT HEK cells, or eGFP fluorescence in Ctrl HEK and CBS HEK cells. (**F**) Mitochondrial ROS levels in BV2 microglia treated with ADT-OH (50 μM) for 8 h or 24 h and then treated with rotenone (Rot), aptenin A5 or malonate (3 independent replicates).

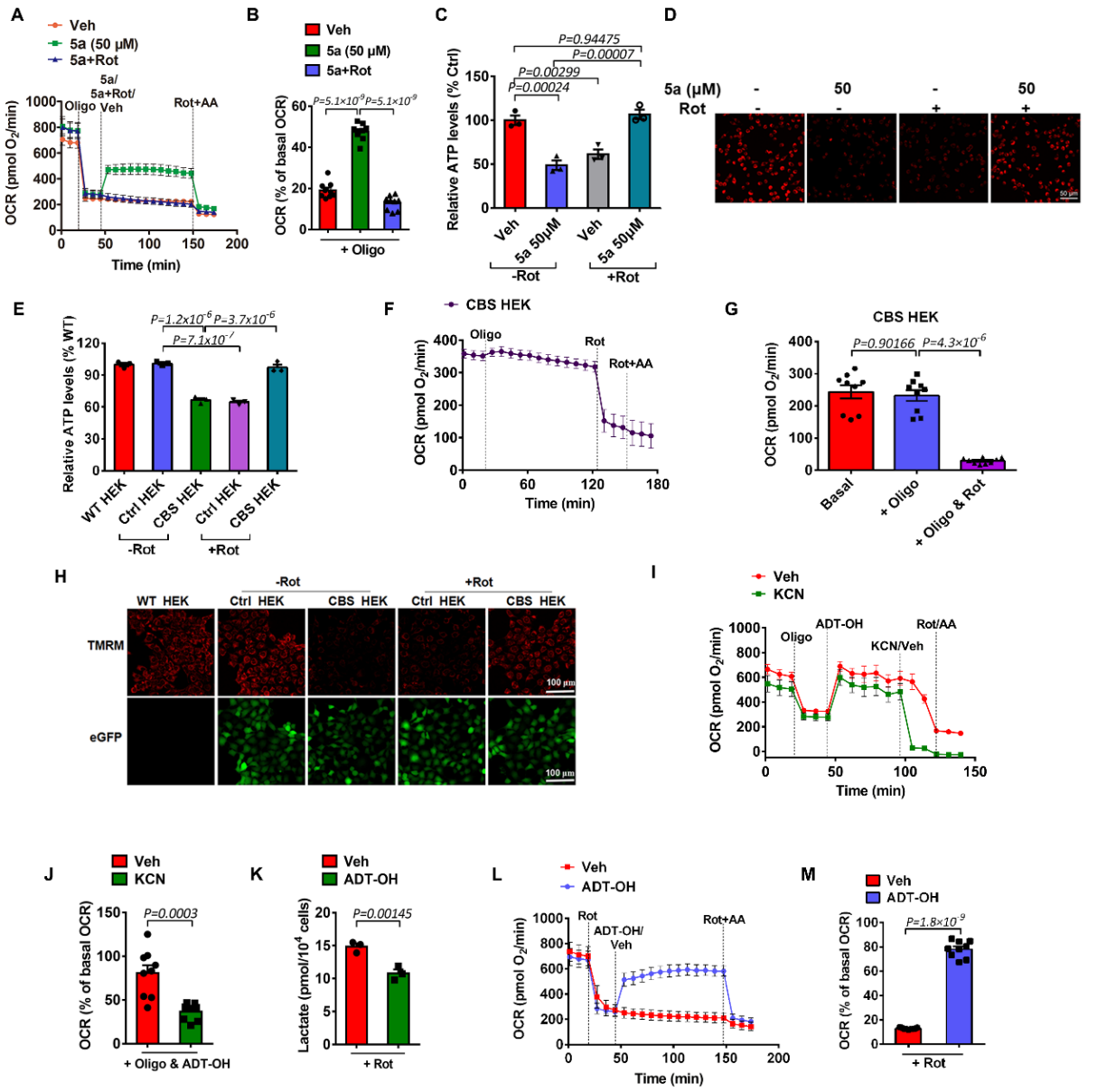
A
Veh
5a (50 µM)
5a+Rot
5a/
5a+Rot/
Veh
Oligo
Rot+AA
OCR (pmol O2/min)
Time (min)
B
Veh
5a (50 µM)
5a+Rot
OCR (% of basal OCR)
+ Oligo
C
Relative ATP levels (% Ctrl)
P=0.94475
P=0.00007
P=0.00299
P=0.00024
Veh
5a 50µM
-Rot
+Rot
D
5a (µM)
Rot
E
Relative ATP levels (% WT)
WT HEK
Ctrl HEK
CBS HEK
-Rot
+Rot
F
CBS HEK
Oligo
Rot
Rot+AA
OCR (pmol O2/min)
Time (min)
G
CBS HEK
P=0.90166
Basal
+ Oligo
+ Oligo & Rot
H
-Rot
+Rot
TMRM
eGFP
100 µm
I
Veh
KCN
Oligo
ADT-OH
KCN/Veh
Rot/AA
OCR (pmol O2/min)
Time (min)
J
Veh
KCN
P=0.0003
OCR (% of basal OCR)
+ Oligo & ADT-OH
K
Veh
ADT-OH
P=0.00145
Lactate (pmol/10^4 cells)
+ Rot
L
Veh
ADT-OH
Rot
ADT-OH/
Veh
Rot+AA
OCR (pmol O2/min)
Time (min)
M
Veh
ADT-OH
P=1.8x10^-9
OCR (% of basal OCR)
+ Rot

Fig. S6. H_2S induces mitochondrial uncoupling via complex I RET. (**A-D**) Abolishment of 5a (50 μM)-induced mitochondrial uncoupling by rotenone (Rot) in BV2 microglia. Mitochondrial uncoupling was indicated by enhanced OCR in the presence of oligomycin (A, real-time change; B, statistical analysis, n = 9), reduced intracellular ATP levels (C, n = 3), and reduced $\Delta\Psi_m$ (D, representative images of TMRM staining from 3 independent replicates). Veh: vehicle. (**E-H**) Rot abolished mitochondrial uncoupling induced by CBS overexpression in HEK293 cells. Mitochondrial uncoupling was indicated by reduced intracellular ATP levels (E, n = 3), enhanced OCR in the presence of oligomycin (F: real-time change; G: statistical analysis; n = 9), and reduced $\Delta\Psi_m$ (H, representative images of TMRM staining; 3 independent experiments). WT HEK: wild-type HEK293 cells; Ctrl HEK: control HEK293 cells expressing eGFP; CBS HEK cells: HEK293 cells overexpressing CBS and eGFP. (**I-J**) The complex IV inhibitor KCN abolished ADT-OH (50 μM)-induced increase in OCR in the presence of oligomycin in BV2 microglia (I, real-time change; J, statistical analysis; n = 9). (**K**) Lactate accumulation in medium collected from BV2 microglia treated with rotenone (Rot) and ADT-OH (50 μM) or Veh for 2 h (n = 3). (**L-M**) Real-time change and quantification of OCR (n = 9) in BV2 microglia treated with Rot and ADT-OH (50 μM) or Veh. Rot, ADT-OH, Veh and AA were added at the indicated timepoints.

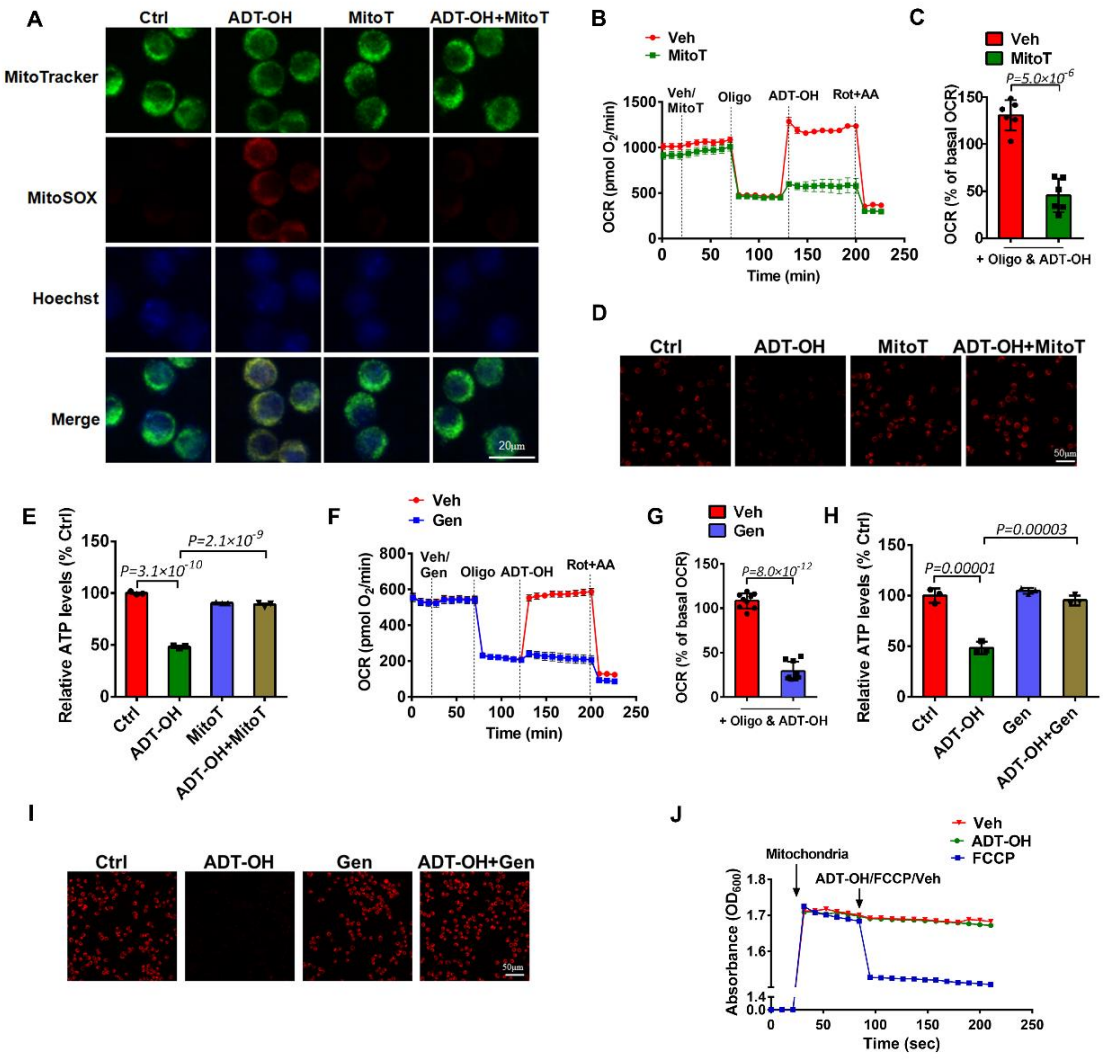
A
Ctrl
ADT-OH
MitoT
ADT-OH+MitoT
MitoTracker
MitoSOX
Hoechst
Merge
20μm
B
Veh
MitoT
Veh/ MitoT
Oligo
ADT-OH
Rot+AA
OCR (pmol O2/min)
Time (min)
C
Veh
MitoT
P=5.0×10-6
OCR (% of basal OCR)
+ Oligo & ADT-OH
D
Ctrl
ADT-OH
MitoT
ADT-OH+MitoT
50μm
E
Relative ATP levels (% Ctrl)
P=3.1×10-10
P=2.1×10-9
Ctrl
ADT-OH
MitoT
ADT-OH+MitoT
F
Veh
Gen
Veh/ Gen
Oligo
ADT-OH
Rot+AA
OCR (pmol O2/min)
Time (min)
G
Veh
Gen
P=8.0×10-12
OCR (% of basal OCR)
+ Oligo & ADT-OH
H
P=0.00001
P=0.00003
Relative ATP levels (% Ctrl)
Ctrl
ADT-OH
Gen
ADT-OH+Gen
I
Ctrl
ADT-OH
Gen
ADT-OH+Gen
50μm
J
Veh
ADT-OH
FCCP
Mitochondria
ADT-OH/FCCP/Veh
Absorbance (OD600)
Time (sec)

Fig. S7. H_2S induces mitochondrial uncoupling via ROS-dependent activation of UCP2. (**A**) Mitochondrial ROS levels in BV2 microglia treated with ADT-OH (50 μM) for 10 min with/without pretreatment with MitoTEMPO (MitoT, 1.5 mM) for 30 min (3 independent replicates). Ctrl: vehicle-treated cells. (**B-E**) Pretreatment with MitoT blocked ADT-OH (50 μM)-induced mitochondrial uncoupling in BV2 microglia, as indicated by OCR (B, real-time change; C, statistical analysis; n = 6), $\Delta\Psi_m$ (D, TMRM staining, 3 independent replicates), and intracellular ATP levels (E, n = 3). Veh: vehicle. (**F-I**) Pretreatment with genipin (Gen) blocked ADT-OH (50 μM)-induced mitochondrial uncoupling in BV2 microglia, as indicated by OCR (F, real-time change; G, statistical analysis; n = 9), intracellular ATP levels (H, n = 3), and $\Delta\Psi_m$ (I, TMRM staining, 3 independent replicates). $\Delta\Psi_m$ and ATP were assessed at 30 min after treatment with ADT-OH and/or MitoT (Gen). (**J**) The assay of swelling of mitochondria isolated from the livers of global SQR knockout mice (representative results from 4 independent replicates). Isolated mitochondria were added to isotonic acetate buffer, followed by addition of vehicle (Veh), ADT-OH (50 μM) or FCCP (1 μM) at the indicated timepoint. Mitochondrial swelling was indicated as a decrease in the absorbance at 600 nm.

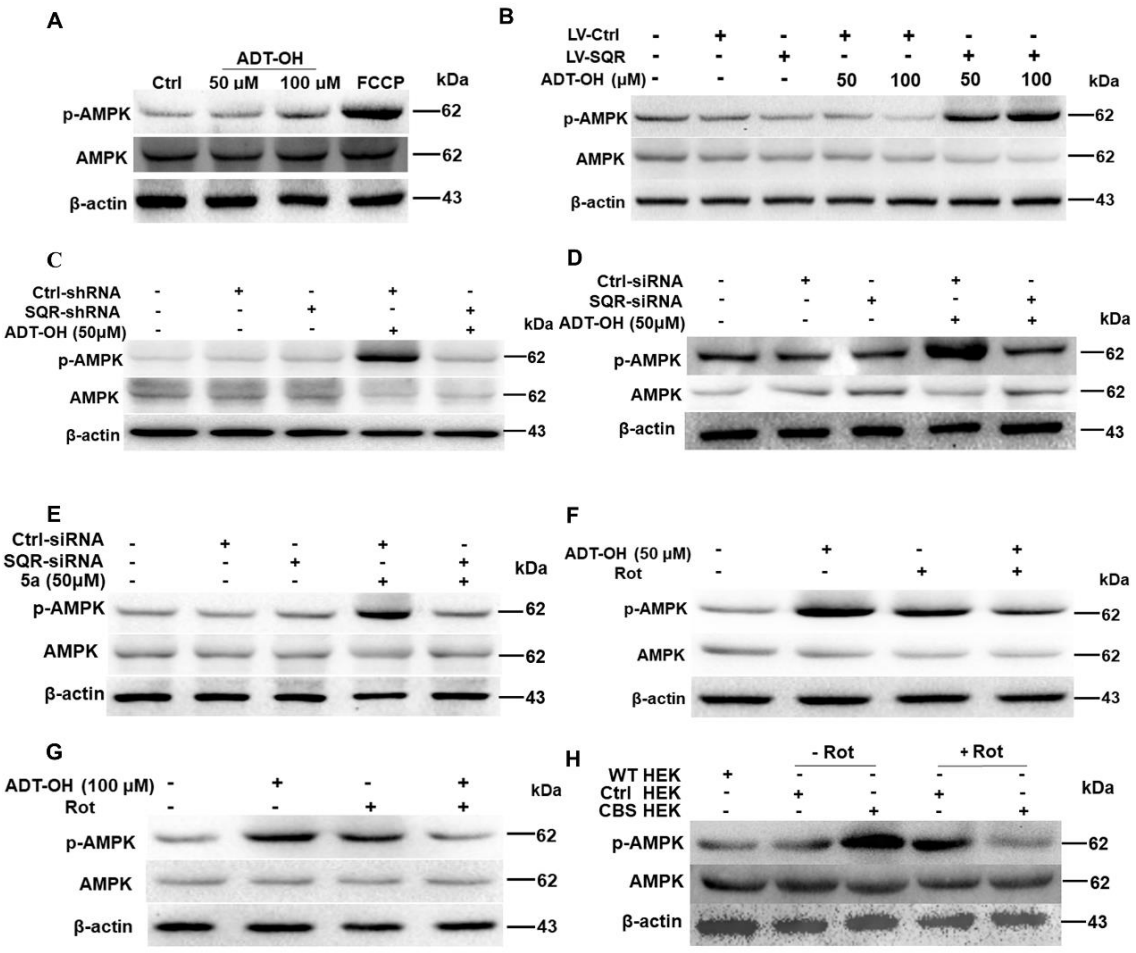
A
ADT-OH
Ctrl
50 μM
100 μM
FCCP
kDa
p-AMPK
AMPK
β-actin
62
62
43
B
LV-Ctrl
LV-SQR
ADT-OH (μM)
50
100
50
100
kDa
C
Ctrl-shRNA
SQR-shRNA
ADT-OH (50μM)
D
Ctrl-siRNA
SQR-siRNA
ADT-OH (50μM)
E
Ctrl-siRNA
SQR-siRNA
5a (50μM)
F
ADT-OH (50 μM)
Rot
G
ADT-OH (100 μM)
Rot
H
- Rot
+ Rot
WT HEK
Ctrl HEK
CBS HEK

Fig. S8. H_2S activates AMPK via SQR-mediated mitochondrial uncoupling. (**A**) AMPK activation indicated by phosphorylation of AMPKα at Thr172 (p-AMPK) in primary neurons treated with ADT-OH or FCCP for 2 h. Ctrl: vehicle-treated cells. (**B**) AMPK activation in primary neurons infected with lentivirus expressing SQR (LV-SQR) or control lentivirus expressing eGFP (LV-Ctrl) for 4 days and then treated with ADT-OH for 2 h. (**C**) AMPK activation in primary microglia infected with lentivirus expressing SQR-shRNA or nonsense shRNA (Ctrl-shRNA) for 4 days and then treated with ADT-OH (50 μM)/Veh for 2 h. (**D-E**) AMPK activation in BV2 microglia transfected with SQR-siRNA or nonsense siRNA (Ctrl-siRNA) for 2 days and then treated with ADT-OH (50 μM) or 5a (50 μM) for 2 h. (**F-G**) AMPK activation in BV2 microglia treated with ADT-OH (50 or 100 μM) and/or Rot for 2 h. (**H**) AMPK activation in WT HEK, Ctrl HEK and CBS HEK cells with/without treatment with Rot for 2 h. For A-H, the experiments were repeated 3 times independently.

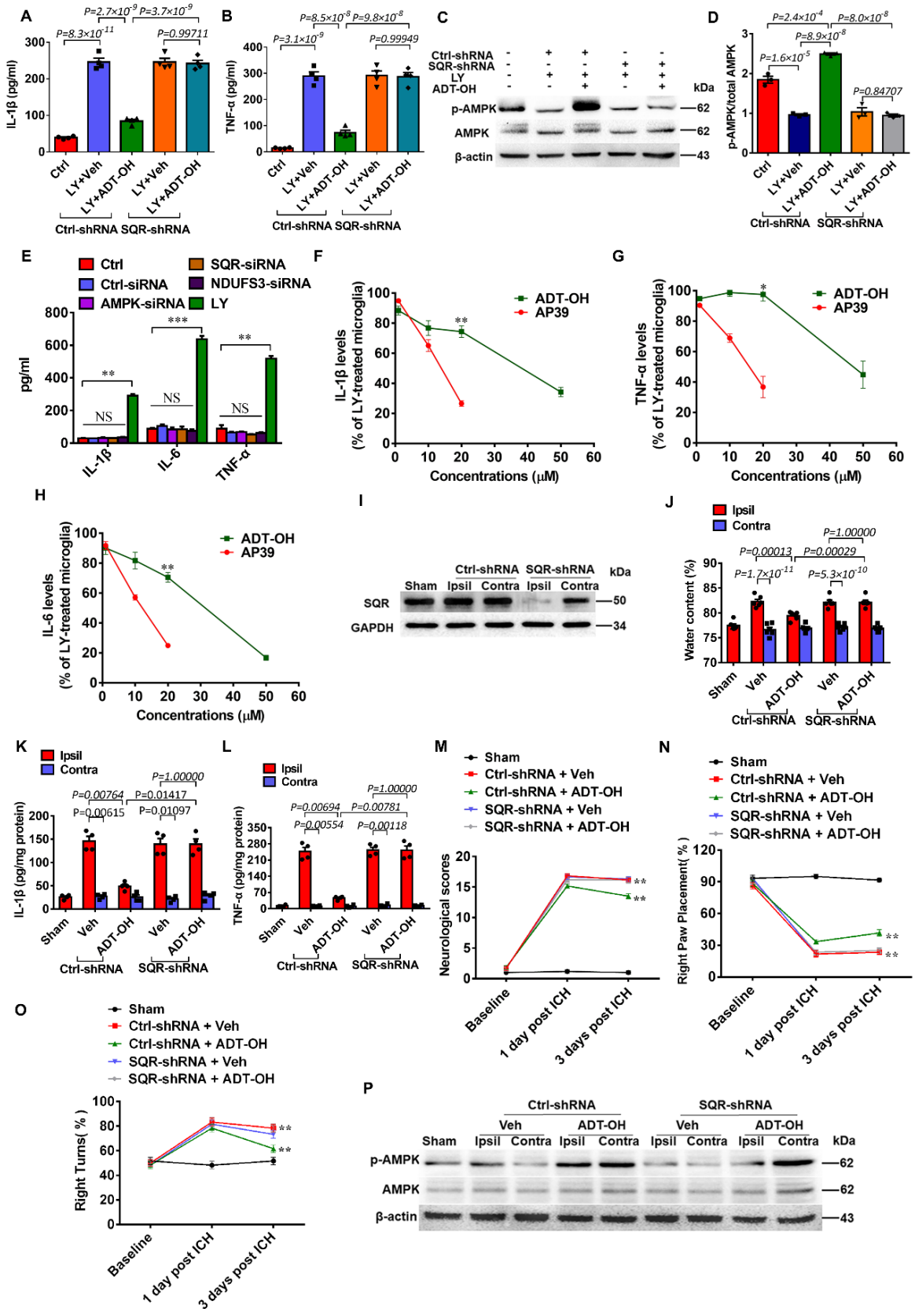
A
B
C
D
E
F
G
H
I
J
K
L
M
N
O
P
IL-1β (pg/ml)
TNF-α (pg/ml)
p-AMPK/total AMPK
Ctrl
LY+Veh
LY+ADT-OH
Ctrl-shRNA
SQR-shRNA
Ctrl-siRNA
SQR-siRNA
AMPK-siRNA
NDUFS3-siRNA
LY
pg/ml
IL-1β
IL-6
TNF-α
NS
ADT-OH
AP39
IL-1β levels (% of LY-treated microglia)
TNF-α levels (% of LY-treated microglia)
IL-6 levels (% of LY-treated microglia)
Concentrations (μM)
p-AMPK
AMPK
β-actin
SQR
GAPDH
kDa
Sham
Ipsil
Contra
Veh
Water content (%)
IL-1β (pg/mg protein)
TNF-α (pg/mg protein)
Ctrl-shRNA + Veh
Ctrl-shRNA + ADT-OH
SQR-shRNA + Veh
SQR-shRNA + ADT-OH
Neurological scores
Right Paw Placement(%)
Right Turns(%)
Baseline
1 day post ICH
3 days post ICH

Fig. S9. SQR knockdown abolishes therapeutic effects of H_2S following ICH. (A-B) Protein levels (n = 4) of IL-1β and TNF-α in primary microglia infected with lentivirus expressing SQR-shRNA or Ctrl-shRNA for 4 days and then treated with red blood cell lysate (LY) and ADT-OH (50 μM) or vehicle (Veh) for 24 h. Ctrl: intact microglia. (**C-D**) Representative images and quantification of AMPK activation in primary microglia infected with lentivirus expressing Ctrl-shRNA or SQR-shRNA for 4 days and then treated with LY and ADT-OH for 2 h (n = 3). (**E**) The siRNA against SQR, AMPK or NDUFS3 did not affect the basal expression of pro-inflammatory mediators in BV2 microglia. (F-H) A comparison of inhibitory effects of AP39 with that of ADT-OH on LY-induced expression of pro-inflammatory mediators in BV2 microglia. **: $p < 0.01$ at the indicated concentration**.** (**I**) SQR expression in the striatum ipsilateral (Ipsil) or contralateral (Contra) to lentiviral injection at 14 days after injection, 3 independent replicates. (**J**) Water content in the striatum at 3 days following ICH (n = 6). Lentivirus expressing SQR-shRNA or Ctrl-shRNA were injected into the left striatum. After 14 days, autologous blood was injecting into the left striatum to induced ICH. Sham: sham-operated mice. (**K-L**) IL-1β and TNF-α levels in the striatum at 3 days following ICH (n = 4). (**M-O)** Neurological deficits assessed by the neurological score, forelimb placement and corner test (n = 6). **, $P < 0.01$, indicating a significant difference between the Ctrl-shRNA-injected mice treated with Veh and ADT-OH (Ctrl-shRNA+Veh vs. Ctrl-shRNA+ADT-OH). No statistical difference detected between SQR-shRNA-injected mice treated with Veh and ADT-OH. (**P**) AMPK activation in the striatum at 3 days following ICH (3 independent replicates).

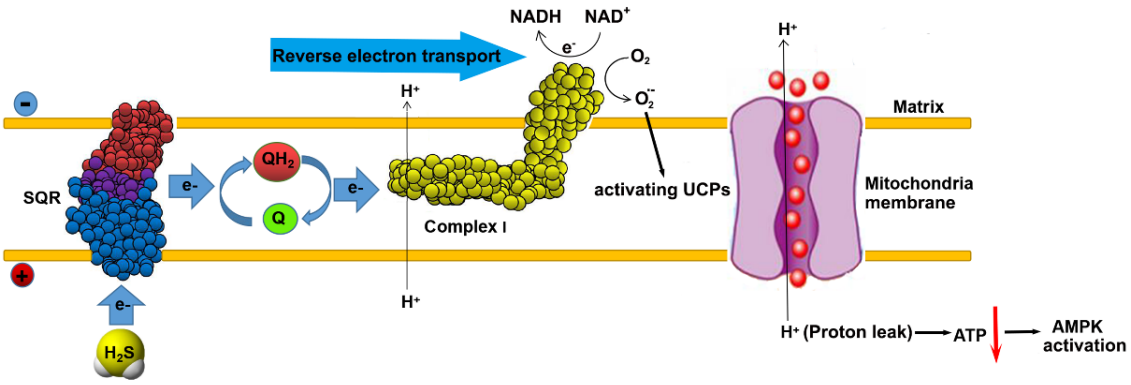

Fig. S10. Proposed mechanism underlying therapeutic actions of H_2S. SQR-mediated oxidation of H_2S initiates mitochondrial ROS generation by driving complex I RET, which in turn induces ROS-dependent mitochondrial uncoupling via uncoupling proteins (e.g. UCP2 or ANT) and consequently activates AMPK.

REFERENCES AND NOTES

1. J. L. Wallace, R. Wang, Hydrogen sulfide-based therapeutics: Exploiting a unique but ubiquitous gasotransmitter. *Nat. Rev. Drug Discov.* **14**, 329–345 (2015).
2. J. L. Wallace, D. Vaughan, M. Dicay, W. K. MacNaughton, G. de Nucci, Hydrogen sulfide-releasing therapeutics: Translation to the clinic. *Antioxid. Redox Signal.* **28**, 1533–1540 (2018).
3. J. L. Wallace, P. Nagy, T. D. Feener, T. Allain, T. Ditrói, D. J. Vaughan, M. N. Muscara, G. de Nucci, A. G. Buret, A proof-of-concept, phase 2 clinical trial of the gastrointestinal safety of a hydrogen sulfide-releasing anti-inflammatory drug. *Br. J. Pharmacol.* **177**, 769–777 (2020).
4. R. Wang, Two's company, three's a crowd: Can H2S be the third endogenous gaseous transmitter? *FASEB J.* **16**, 1792–1798 (2002).
5. B. D. Paul, S. H. Snyder, H_2S signalling through protein sulfhydration and beyond. *Nat. Rev. Mol. Cell Biol.* **13**, 499–507 (2012).
6. J. T. Hancock, M. Whiteman, Hydrogen sulfide and cell signaling: Team player or referee? *Plant Physiol. Biochem.* **78**, 37–42 (2014).
7. F. Bouillaud, F. Blachier, Mitochondria and sulfide: A very old story of poisoning, feeding, and signaling? *Antioxid. Redox Signal.* **15**, 379–391 (2011).
8. E. Lagoutte, S. Mimoun, M. Andriamihaja, C. Chaumontet, F. Blachier, F. Bouillaud, Oxidation of hydrogen sulfide remains a priority in mammalian cells and causes reverse electron transfer in colonocytes. *Biochim. Biophys. Acta* **1797**, 1500–1511 (2010).
9. M. Goubern, M. Andriamihaja, T. Nübel, F. Blachier, F. Bouillaud, Sulfide, the first inorganic substrate for human cells. *FASEB J.* **21**, 1699–1706 (2007).
10. E. T. Chouchani, V. R. Pell, E. Gaude, D. Aksentijević, S. Y. Sundier, E. L. Robb, A. Logan, S. M. Nadtochiy, E. N. Ord, A. C. Smith, F. Eyassu, R. Shirley, C.-H. Hu, A. J. Dare, A. M. James, S. Rogatti, R. C. Hartley, S. Eaton, A. S. Costa, P. S. Brookes, S. M. Davidson, M. R. Duchen, K. Saeb-Parsy, M. J. Shattock, A. J. Robinson, L. M. Work, C. Frezza, T. Krieg, M. P. Murphy, Ischaemic accumulation of succinate controls reperfusion injury through mitochondrial ROS. *Nature* **515**, 431–435 (2014).
11. E. L. Mills, B. Kelly, A. Logan, A. S. Costa, M. Varma, C. E. Bryant, P. Tourlomousis, J. H. Däbritz, E. Gottlieb, I. Latorre, S. C. Corr, G. McManus, D. Ryan, H. T. Jacobs, M. Szibor, R. J. Xavier, T. Braun, C. Frezza, M. P. Murphy, L. A. O'Neill, Succinate dehydrogenase supports metabolic repurposing of mitochondria to drive inflammatory macrophages. *Cell* **167**, 457–470.e13 (2016).

12. F. Scialò, A. Sriram, D. Fernández-Ayala, N. Gubina, M. Lõhmus, G. Nelson, A. Logan, H. M. Cooper, P. Navas, J. A. Enríquez, M. P. Murphy, A. Sanz, Mitochondrial ROS produced via reverse electron transport extend animal lifespan. *Cell Metab.* **23**, 725–734 (2016).
13. E. L. Robb, A. R. Hall, T. A. Prime, S. Eaton, M. Szibor, C. Viscomi, A. M. James, M. P. Murphy, Control of mitochondrial superoxide production by reverse electron transport at complex I. *J. Biol. Chem.* **293**, 9869–9879 (2018).
14. H. Kong, N. S. Chandel, Regulation of redox balance in cancer and T cells. *J. Biol. Chem.* **293**, 7499–7507 (2018).
15. K. S. Echtay, D. Roussel, J. St-Pierre, M. B. Jekabsons, S. Cadenas, J. A. Stuart, J. A. Harper, S. J. Roebuck, A. Morrison, S. Pickering, J. C. Clapham, M. D. Brand, Superoxide activates mitochondrial uncoupling proteins. *Nature* **415**, 96–99 (2002).
16. E. L. Mills, K. A. Pierce, M. P. Jedrychowski, R. Garrity, S. Winther, S. Vidoni, T. Yoneshiro, J. B. Spinelli, G. Z. Lu, L. Kazak, A. S. Banks, M. C. Haigis, S. Kajimura, M. P. Murphy, S. P. Gygi, C. B. Clish, E. T. Chouchani, Accumulation of succinate controls activation of adipose tissue thermogenesis. *Nature* **560**, 102–106 (2018).
17. H. Tao, Y. Zhang, X. Zeng, G. I. Shulman, S. Jin, Niclosamide ethanolamine–induced mild mitochondrial uncoupling improves diabetic symptoms in mice. *Nat. Med.* **20**, 1263–1269 (2014).
18. R. J. Perry, D. Zhang, X.-M. Zhang, J. L. Boyer, G. I. Shulman, Controlled-release mitochondrial protonophore reverses diabetes and steatohepatitis in rats. *Science* **347**, 1253–1256 (2015).
19. X. Zhou, Y. Cao, G. Ao, L. Hu, H. Liu, J. Wu, X. Wang, M. Jin, S. Zheng, X. Zhen, N. J. Alkayed, J. Jia, J. Cheng, CaMKKβ-dependent activation of AMP-activated protein kinase is critical to suppressive effects of hydrogen sulfide on neuroinflammation. *Antioxid. Redox Signal.* **21**, 1741–1758 (2014).
20. M. Lee, V. Tazzari, D. Giustarini, R. Rossi, A. Sparatore, P. Del Soldato, E. McGeer, P. L. McGeer, Effects of hydrogen sulfide-releasing L-DOPA derivatives on glial activation: Potential for treating Parkinson disease. *J. Biol. Chem.* **285**, 17318–17328 (2010).
21. Y. Zhao, H. Wang, M. Xian, Cysteine-activated hydrogen sulfide (H_2S) donors. *J. Am. Chem. Soc.* **133**, 15–17 (2011).
22. S. Mimoun, M. Andriamihaja, C. Chaumontet, C. Atanasiu, R. Benamouzig, J. M. Blouin, D. Tomé, F. Bouillaud, F. Blachier, Detoxification of H_2S by differentiated colonic epithelial cells: Implication of the sulfide oxidizing unit and of the cell respiratory capacity. *Antioxid. Redox Signal.* **17**, 1–10 (2012).

23. E. T. Chouchani, V. R. Pell, A. M. James, L. M. Work, K. Saeb-Parsy, C. Frezza, T. Krieg, M. P. Murphy, A unifying mechanism for mitochondrial superoxide production during ischemia-reperfusion injury. *Cell Metab.* **23**, 254–263 (2016).
24. S. Lee, E. Tak, J. Lee, M. A. Rashid, M. P. Murphy, J. Ha, S. S. Kim, Mitochondrial H_2O_2 generated from electron transport chain complex I stimulates muscle differentiation. *Cell Res.* **21**, 817–834 (2011).
25. P. Hernansanz-Agustín, E. Ramos, E. Navarro, E. Parada, N. Sánchez-López, L. Peláez-Aguado, J. D. Cabrera-García, D. Tello, I. Buendia, A. Marina, J. Egea, M. G. López, A. Bogdanova, A. Martínez-Ruiz, Mitochondrial complex I deactivation is related to superoxide production in acute hypoxia. *Redox Biol.* **12**, 1040–1051 (2017).
26. P. G. Roberts, J. Hirst, The deactive form of respiratory complex I from mammalian mitochondria is a Na^+/H^+ antiporter. *J. Biol. Chem.* **287**, 34743–34751 (2012).
27. A. Longchamp, T. Mirabella, A. Arduini, M. R. MacArthur, A. Das, J. H. Treviño-Villarreal, C. Hine, I. Ben-Sahra, N. H. Knudsen, L. E. Brace, J. Reynolds, P. Mejia, M. Tao, G. Sharma, R. Wang, J.-M. Corpataux, J.-A. Haefliger, K. H. Ahn, C.-H. Lee, B. D. Manning, D. A. Sinclair, C. S. Chen, C. K. Ozaki, J. R. Mitchell, Amino acid restriction triggers angiogenesis via GCN2/ATF4 regulation of VEGF and H_2S production. *Cell* **173**, 117–129.e14 (2018).
28. R. De Simone, M. A. Ajmone-Cat, M. Pandolfi, A. Bernardo, C. De Nuccio, L. Minghetti, S. Visentin, The mitochondrial uncoupling protein-2 is a master regulator of both M1 and M2 microglial responses. *J. Neurochem.* **135**, 147–156 (2015).
29. C.-Y. Zhang, L. E. Parton, C. P. Ye, S. Krauss, R. Shen, C.-T. Lin, J. A. Porco Jr., B. B. Lowell, Genipin inhibits UCP2-mediated proton leak and acutely reverses obesity- and high glucose-induced β cell dysfunction in isolated pancreatic islets. *Cell Metab.* **3**, 417–427 (2006).
30. N. Kanemoto, T. Okamoto, K. Tanabe, T. Shimada, H. Minoshima, Y. Hidoh, M. Aoyama, T. Ban, Y. Kobayashi, H. Ando, Y. Inoue, M. Itotani, S. Sato, Antidiabetic and cardiovascular beneficial effects of a liver-localized mitochondrial uncoupler. *Nat. Commun.* **10**, 2172 (2019).
31. M. Wang, W. Tang, Y. Z. Zhu, An update on AMPK in hydrogen sulfide pharmacology. *Front. Pharmacol.* **8**, 810 (2017).
32. E. C. Hinchy, A. V. Gruszczyk, R. Willows, N. Navaratnam, A. R. Hall, G. Bates, T. P. Bright, T. Krieg, D. Carling, M. P. Murphy, Mitochondria-derived ROS activate AMP-activated protein kinase (AMPK) indirectly. *J. Biol. Chem.* **293**, 17208–17217 (2018).

33. Y. P. Zhu, J. R. Brown, D. Sag, L. Zhang, J. Suttles, Adenosine 5’-monophosphate–activated protein kinase regulates IL-10–mediated anti-inflammatory signaling pathways in macrophages. *J. Immunol.* **194**, 584–594 (2015).
34. Y. Zhou, Y. Wang, J. Wang, R. Anne Stetler, Q.-W. Yang, Inflammation in intracerebral hemorrhage: From mechanisms to clinical translation. *Prog. Neurobiol.* **115**, 25–44 (2014).
35. Y.-C. Wang, Y. Zhou, H. Fang, S. Lin, P.-F. Wang, R.-P. Xiong, J. Chen, X.-Y. Xiong, F.-L. Lv, Q.-L. Liang, Q.-W. Yang, Toll-like receptor 2/4 heterodimer mediates inflammatory injury in intracerebral hemorrhage. *Ann. Neurol.* **75**, 876–889 (2014).
36. C. Hine, E. Harputlugil, Y. Zhang, C. Ruckenstuhl, B. C. Lee, L. Brace, A. Longchamp, J. H. Treviño-Villarreal, P. Mejia, C. K. Ozaki, R. Wang, V. N. Gladyshev, F. Madeo, W. B. Mair, J. R. Mitchell, Endogenous hydrogen sulfide production is essential for dietary restriction benefits. *Cell* **160**, 132–144 (2015).
37. A. M. Bertholet, E. T. Chouchani, L. Kazak, A. Angelin, A. Fedorenko, J. Z. Long, S. Vidoni, R. Garrity, J. Cho, N. Terada, D. C. Wallace, B. M. Spiegelman, Y. Kirichok, H^+ transport is an integral function of the mitochondrial ADP/ATP carrier. *Nature* **571**, 515–520 (2019).
38. K. Umemura, H. Kimura, Hydrogen sulfide enhances reducing activity in neurons: Neurotrophic role of H_2S in the brain? *Antioxid. Redox Signal.* **9**, 2035–2041 (2007).
39. K. Módis, C. Coletta, K. Erdélyi, A. Papapetropoulos, C. Szabo, Intramitochondrial hydrogen sulfide production by 3-mercaptopyruvate sulfurtransferase maintains mitochondrial electron flow and supports cellular bioenergetics. *FASEB J.* **27**, 601–611 (2013).
40. G. Huang, Y. Chen, H. Lu, X. Cao, Coupling mitochondrial respiratory chain to cell death: An essential role of mitochondrial complex I in the interferon-β and retinoic acid-induced cancer cell death. *Cell Death Differ.* **14**, 327–337 (2007).